Correlating the Kinetics of Cytokine-Induced E-Selectin Adhesion and Expression on Endothelial Cells

J. Dora Levin, H. Ping Ting-Beall, and Robert M. Hochmuth
Department of Mechanical Engineering and Materials Science, Duke University, Durham, North Carolina 27708-0300 USA

ABSTRACT Many human diseases are mediated through the immune system. In chronic inflammatory disorders, the processes ordinarily involved in tissue healing become destructive. Endothelial cells normally recruit leukocytes to inflamed tissue using cytokine-induced adhesion receptors on the surfaces of interacting cells. Leukocyte capture depends on specialized characteristics of these receptors, particularly the binding kinetics. This study is designed to clarify the relationship between cytokine-induced changes in cell properties and binding kinetics. Here, we measure the kinetics of expression and monoclonal antibody binding for E-selectin in interleukin-1α-stimulated microvascular endothelium in vitro and incorporate the data into kinetic models. Quantitative flow cytometry is used to determine molecular density (expression), and micropipette assays are used to find the probability of adhesion (function). Within five hours of interleukin-1α stimulation, E-selectin density increases from 0 to 742 sites/μm^2, and antibody-E-selectin adhesion probability increases from a baseline of 6.3% to 64%. A kinetic model is applied to find an apparent association rate constant, k_f, of 3.7×10^{-14} cm^2/sec for antibody-E-selectin binding. Although the model successfully predicts experimental results, the rate constant is undervalued for a diffusion-limited process, suggesting that functional adhesion may be modified through cytokine-induced changes in microtopology and receptor localization.

INTRODUCTION

The endothelium actively recruits leukocytes to sites of inflammation. Cytokine-stimulated endothelial cells (EC) bind chemoattractant-activated leukocytes through receptor-mediated adhesion. Several effective models have been used to characterize and differentiate the roles of adhesion receptors in the finely tuned, multistep process of transendothelial migration (Kansas, 1996; Lu et al., 1997; Lynam et al., 1998; Marlin and Springer, 1987; Neelamegham et al., 1998; Tonnesen et al., 1989). The selectins are characterized by rapid rates of association and dissociation, ideal kinetic qualities for initiating attachment under flow (Abbassi et al., 1993; Alon et al., 1996, 1997; Chen et al., 1997; Kansas, 1996; Puri et al., 1997; Smith et al., 1999). Cytokine-inducible E-selectin on EC mediates initial leukocyte rolling, attachment, and paracrine or contact activation of leukocytes (Kansas, 1996; Kuijpers et al., 1991). Cytokine-stimulated EC secrete chemokines (i.e., IL-8 and platelet-activating factor) which induce neutrophil diapedesis through concomitant changes in adhesion receptor surface expression and activation, and changes in morphology (Erlandsen et al., 1993; Huber et al., 1991; Kuijpers et al., 1991; Macconi et al., 1995; Smith et al., 1991). Neutrophils express several putative ligands for E-selectin including: E-selectin-ligand-1 (ESL-1) (Levinovitz et al., 1993; Steegmaier et al., 1995), P-selectin ligand-1 (PSGL-1) (Patel et al., 1995; Sako et al., 1993), sialyl Lewis x carbohydrate (sLe^x), and possibly L-selectin (Kansas, 1996; Tedder et al., 1995). However, there is some ambiguity as to the distinct functional roles for these ligands during E-selectin-mediated leukocyte rolling (Alon et al., 1996; Patel and McEver, 1997; Yang et al., 1999). Leukocyte transport from circulation to tissue depends on how strongly and rapidly surface receptors bind to their ligands under a variety of hemodynamic, environmental, temporal, and topological conditions.

Few studies have quantified kinetic binding rates with both receptors confined to surfaces (two-dimensional kinetics), although these parameters are fundamental determinants of intercellular adhesion. Increasing numbers of investigators use micromechanical approaches to measure adhesion strength and kinetic rate constants, such as centrifugation assays (Piper et al., 1998), shear flow chambers (Kaplanski et al., 1993; Smith et al., 1999), cone and plate viscometry (Lynam et al., 1998; Neelamegham et al., 1998), atomic force microscopy (Fritz et al., 1998; Merkel et al., 1999), and micromanipulation (Chesla et al., 1998; Evans et al., 1995). This is the first investigation in which adhesion kinetics are measured for a native adhesion receptor, E-selectin, in cultured EC under physiological conditions. Recent work by Chesla et al. (1998) includes the development of a theoretical framework for the micropipette adhesion assay that emphasizes the kinetic relationships between imposed constraints and physical measurements. Calculations of forward and reverse kinetic rate constants require accurate values for receptor density, contact area, and duration, and in some cases the force applied to the bond (Bell, 1978). In the in vitro flow models, analyses rely on capture rates, collision frequencies, pause times, and rolling velocities with highly variable contact force, area, and duration

Received for publication 2 February 2000 and in final form 21 November 2000.

Address reprint requests to Robert M. Hochmuth, Department of Mechanical Engineering and Materials Science, Duke University, Durham, NC 27708-0300. Tel.: 919-660-5307; Fax: 919-660-8963; E-mail: hochmuth@acpub.duke.edu. Dr. Levin's present address is Department of Biomedical Engineering, Duke University, Durham, NC 27708-0281.

0006-3495/01/02/656/12 $2.00

(Alon et al., 1997; Chen et al., 1997; Kaplanski et al., 1993; Smith et al., 1999). The micropipette adhesion assay used here has distinct advantages for precise application of forces, contact area, and duration for each surface collision (Chesla et al., 1998; Shao and Hochmuth, 1996).

Intercellular adhesion is mediated through a variety of receptors with unique physical and kinetic characteristics, regulatory patterns, and tissue or cell localization well suited for their diverse functions. In this study, we adapt micropipette adhesion assays to measure the kinetics of adhesion receptor E-selectin binding on passive and cytokine-activated microvascular EC (MVEC). Due to the cascade of signaling molecules induced by cytokine exposure and receptor mediated binding, monoclonal antibody (mAb)-coated microspheres are used instead of neutrophils to probe functional receptor binding without the ambiguity of heterogeneous receptor adhesion. mAb-coated microspheres are used to probe the surface of IL-1α-stimulated MVEC to specifically measure E-selectin adhesion probability (P_a). Quantitative flow cytometry measurements characterize the rate of expression and surface density of E-selectin on passive and cytokine-stimulated MVEC and the surface density of mAb on the microsphere probes. The data are incorporated into probabilistic kinetic models of receptor–ligand binding. Nonlinear fit parameters are used to derive association rate constants for mAb binding to E-selectin. With membrane-bound interacting species, the association rate constant, k_f, depends on membrane transport to bring reacting proteins into encounter distance and the intrinsic reaction rate to form a bond. Because lateral diffusion rates are typically much slower than intrinsic binding reactions for proteins in lipid membranes, whether for receptor–ligand or antibody (Ab)–antigen interactions, we hypothesize that k_f is diffusion limited (Jacobson et al., 1987; Lauffenburger and Linderman, 1993; Webb et al., 1981). The results presented here validate this assumption, but also contribute to the development of quantitative assays and the integration of quantitative kinetic data. The results show that the micropipette adhesion assay is sensitive to changes in receptor density, but the difference between the expected and calculated rate constants implies additional effects, possibly due to surface structure.

MATERIALS AND METHODS

Cell culture

Human lung MVEC (MVEC-L; Clonetics, San Diego, CA) are cultivated in endothelial growth media for MVEC-L (EGM2-MV; Clonetics) through passage eight in tissue culture flasks at 37°C and with 5% CO_2. Cells are harvested using standard trypsin/EDTA enzymatic cell dissociation. Dermal MVEC (MVEC-d; Clonetics), used to determine the effects of eliminating serum or growth factors from the media, are grown in endothelial growth media for MVEC-d (Clonetics), through passage five. MVEC are stored long-term in liquid nitrogen in media containing 10% FBS and 10% DMSO.

For micropipette adhesion assays, cells are grown onto microcarriers to create a cell surface that is accessible both physically and optically. Microcarrier cell culture methods are adapted from established techniques (Davies, 1981; Davies and Kerr, 1982). In brief, dry collagen-coated dextran microcarrier beads (Cytodex 3; Pharmacia Biotech, Piscataway, NJ) with a mean 150-μm diameter are hydrated for 3 h in Dulbecco's phosphate-buffered saline without Ca^{2+} or Mg^{2+} (DPBS; Gibco BRL, Gaithersburg, MD) with 0.1% Tween 80 (Sigma, St. Louis, MO) to reduce surface tension. The microcarriers are washed twice with 70% ethanol, soaked overnight to sterilize, washed three times in DPBS, and stored at a 10^5 microcarrier/mL concentration. Before cell transfer, microcarriers are washed in modified EGM2-MV (15 mM HEPES, 5% cell culture grade bovine serum albumin (Sigma), pH 7.2–7.4) and inoculated with MVEC-L at a 20:1 (cells:beads) ratio. Monolayers of MVEC-L grow to confluence on microcarriers at 37°C and with 5% CO_2 within 5–7 days in culture (Fig. 1). For electron microscopy, MVEC-L are grown onto 160–300-μm diameter latex microcarriers (Biosilon, Nalge Nunc International, Naperville, IL).

Quantitative flow cytometry

Quantitative flow cytometry is used to determine the surface density of receptors on MVEC and the number of saturable Ab binding sites on the surface of microspheres. Background fluorescence, autofluorescence combined with nonspecific binding of Ab, is determined using an isotype control, phycoerythrin (PE)-labeled mouse Ab (MOPC-31C IgG_1-PE; Ancell, Bayport, MN).

Nonenzymatic cell harvest

For flow cytometry, to prevent receptor hydrolysis by trypsin, cells are harvested using a nonenzymatic detachment method. For the experiments involving cytokines, confluent monolayers of MVEC are grown in tissue culture flasks and incubated with 0–300 U/mL IL-1α (Sigma) for up to 5 h before cell detachment. All detachment buffers are chilled at 4°C and contain 0.1% sodium azide to minimize protein degradation. Confluent flasks are washed twice and immersed in ice-cold EDTA buffer (2% Na·EDTA in DPBS) for 10 min, inducing the cells to round up. The cells

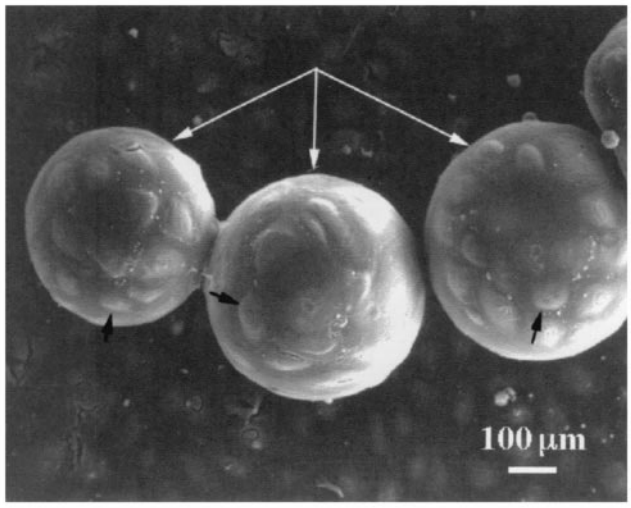

FIGURE 1 Scanning electron micrograph (SEM) of a confluent monolayer of MVEC-L (*black arrows*) grown onto latex microcarriers (*white arrows*). Samples were prepared as described in Shao et al. (1998), but dehydration series were carried out using ethanol instead of acetone.

are removed from the substrate using 37°C Cell Dissociation Solution (Sigma) for 5–10 min. The flask is rapped gently to remove strongly adherent cells. The cells are washed in 2% BSA in DPBS (DB buffer) and counted using trypan blue exclusion to determine cell viability (>95% viable). Samples are suspended in DB buffer and normalized for the number of cells in each sample.

Cell and microsphere labeling

MVEC are incubated with IgG_1 mAb anti-human E-selectin, PE conjugated (anti-E-selectin-PE; Ancell), or an equivalent mass of IgG_1-PE for 45 min in the dark at 4°C. All samples are washed with DB buffer and fixed in 1.0% paraformaldehyde (Aldrich, Milwaukee, WI). To determine the site density of bound Ab on saturated microspheres, the microspheres are incubated with 0.4–20 μg/ml (0.04–2 μg) of anti-E-selectin-PE for one h at 37°C, or with 0.4–50 μg/ml (0.04–5 μg) of isotype control with FITC-labeled mouse Ab (MOPC-31C IgG_1-FITC; Ancell) overnight at 4°C, washed with DB buffer, and measured using quantitative flow cytometry.

Cytometer calibration

Quantum Simply Cellular site density calibration standards, five sets of latex beads with increasing numbers of covalently bound mAb binding sites (0–298,000), are incubated with saturating amounts of fluorophore-conjugated Ab, either anti-E-selectin-PE, IgG_1-PE, or IgG_1-FITC depending on which cell or microsphere marker is calibrated. Signals from bound Ab are measured using a FACScan or FACStar Plus flow cytometer (Becton Dickinson, San Jose, CA). On the histogram plot of events per fluorescent intensity, each population of beads results in a distinct peak (Fig. 2 *A*). The statistics for these peaks (Table 1) are used to find the linear relationship between mean intensity and the number of bound Ab sites per sphere (Fig. 2 *B*). This relationship is used to translate the measured mean fluorescent intensity to a number of bound antigen or secondary Ab sites in any sample of cells or microspheres.

Flow cytometry data analysis

Typically, data are collected for 10,000 cells for each set of flow cytometry experiments. Data are compensated for background fluorescence by subtracting the mean fluorescent intensity or mean number of receptors found using the isotype control. Cells having intensity greater than the 95th percentile of the isotype control are defined as receptor-positive.

Antibody-coated probe preparation

Microsphere probes are prepared using 10-μm diameter latex microspheres (Sigma) with covalently bound goat anti-mouse IgG Ab. Two drops of well-mixed microspheres are washed twice in DPBS. The microspheres are incubated with saturating concentrations of the primary mAb anti-human E-selectin IgG_1 (Chemicon, Temucula, CA), for one h at 37°C while being gently stirred. The Ab-coated microspheres are washed twice in DPBS to remove excess Ab. For some control experiments, microspheres are washed without adding primary mAb.

Micropipette adhesion measurements

The micropipette adhesion assay is adapted from the methods developed by Shao and Hochmuth (1996) and Chesla et al. (1998).

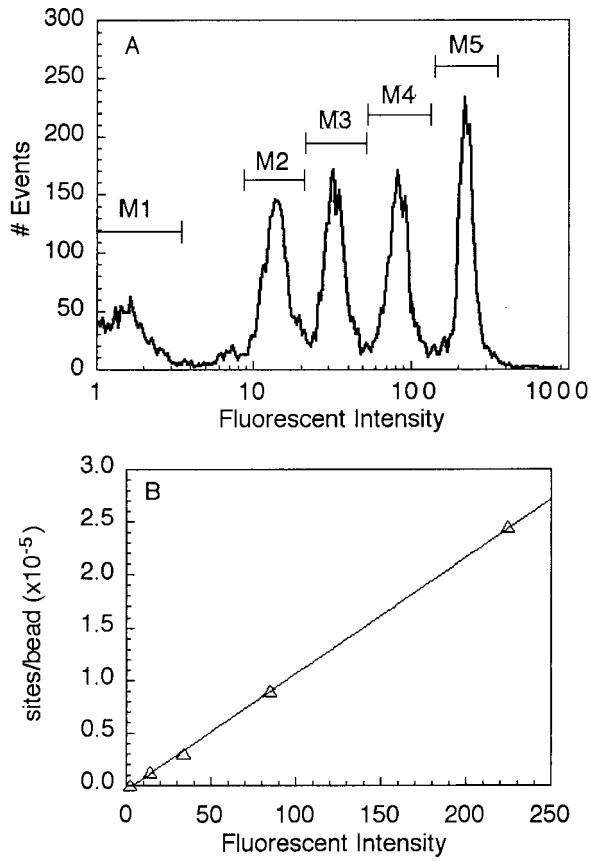

FIGURE 2 Molecular site density calibration. (A) Histogram shows intensity of labeled beads, measured by flow cytometry. Each region, M1-M5, defines a set of beads. (B) The statistics for each region (Table 1) are used to find the linear relationship between the number of bound fluorescent Ab sites (#) per bead and the mean fluorescent intensity (FL), for example # = 1110*FL - 4080, R = 1. The relationship for each Ab marker is used to calculate the molecular density of receptors on the surface of labeled cells or beads.

Micropipette preparation

Micropipettes are prepared by heating and pulling a glass tube (0.75 × 0.4 × 15.2 mm; A-M Systems, Inc., Everett, WA) using a weighted, vertical pipette puller (Model 700C; David Kopf Instruments, Tujunga, CA). The tips of micropipettes used to manipulate the microsphere probes (probing micropipette) are cut using a microforge to produce a smooth 10-μm inner-diameter opening. The micropipettes used to stabilize microcarriers (holding micropipette) are cut with a diamond-tipped glass scribe

TABLE 1 Typical flow cytometry calibration data

Marker (sites)	Events	% Total	FL, Mean*	FL, SD*
M1 (blank)†	1748	20	2	0.58
M2 (12,500)	1843	20	14	2.75
M3 (30,000)	1783	20	34	6.17
M4 (90,000)	1782	20	85	15.28
M5 (245,000)	1760	20	225	33.02

*Statistics for histogram regions M1–M5.
†M1 has no IgG binding sites, M2 has 12,500 binding sites per bead, etc.

and are fire-hardened to create a smooth 100–140-μm opening. Each micropipette is filled with sterile filtered 0.9% NaCl. Before each experiment, micropipettes are attached to micromanipulators and allowed to incubate in modified EGM2-MV under a slight negative pressure for 30–45 min to coat the tips and minimize sticking.

Micropipette manipulation apparatus

The apparatus used in these experiments is similar to the one described by Shao and Hochmuth (1996), with modifications for the manipulation of MVEC-L-confluent microcarriers. The adhesion measurements are observed using a Leitz inverted microscope with a Zeiss planapo 40×, 1.0 N.A. oil-immersion objective and a 15× eyepiece. Images are collected through a charge-coupled device (CCD) camera (model XC-77; Hamamatsu, Tokyo, Japan) coupled to a digital voltage multiplexer (model 401; Vista Electronics, Ramona, CA). The video image and time are displayed on a monitor in real time and recorded for later analysis.

The pressure across each micropipette tip is adjusted by raising and lowering the attached reservoir, roughly using a rack-and-pinion screw or precisely using a manometer with 10-μm vertical resolution, which corresponds to a 0.1 pN/μm^2 pressure difference. Clusters of MVEC-L-confluent microcarriers are aspirated onto the tip of a holding micropipette and stabilized by lowering the microcarriers to the bottom of the chamber. To minimize injury to the monolayer by the micropipette, the clusters are held by a microcarrier distal from the surface being probed for adhesion. The temperature (37°C) and pH (7.4) of the media are regulated throughout the experiments. Experiments are performed with optimum levels of cytokine, so that evaporation does not induce a dose response in addition to temporal changes in cytokine-induced receptor expression. The probing micropipette is used to pick up a snugly-fitting microsphere probe.

Micropipette adhesion assay

MVEC-L surfaces are tested for receptor-mediated adhesion with either Ab-coated microsphere probes (Fig. 3 *A*) or uncoated (goat anti-mouse) microspheres. The motion of the probe is controlled precisely using regulated suction and ejection of the probing micropipette fluid (Fig. 3, *B–E*). The pressure difference across the probe is "zeroed" periodically, every few minutes, to compensate for evaporation and changes in curvature at the media/air interface (Fig. 3 *B*). The 2-pN/μm^2 pressure drop across the probe, p_{a-}, is applied using the manometer (Fig. 3 *C*). The free velocity of the probe, v_f, is proportional to the applied pressure and is observed without adhesion. A small positive pressure difference, p_{a+}, is applied by increasing the air pressure in the reservoir to force the probe to gently contact the cell surface (Fig. 3 *D*). After surface contact, the positive applied pressure is released, returning the system to the applied negative-pressure difference (Fig. 3 *E*). The cell is probed repeatedly for several minutes with a single probe/cell pair before sampling another cell or with another bead.

Adhesion data analysis

The microsphere probe motion is recorded on video tape at 60 fields/s for later analysis. The tapes are carefully analyzed in real time and in slow motion, with each touch scored as "0", for contact without adhesion (Fig. 3 *F*, *mode 1*), or "1", for adhesion events (Fig. 3 *F*, *mode 2* or *3*). The time is recorded for each adhesion event. Cumulative adhesion events are tallied against the total number of touches, elapsed time, and elapsed time from cytokine addition. The contact area, A_c (μm^2), is estimated from video micrographs using a calibrated video caliper to measure the contact diameter as delineated by separation of surfaces at contact. The contact time, t_c (sec), is measured by tracking the number of video fields that the two surfaces remain in contact and multiplying by the time lapse per field (1/60 sec). For each adhesion assay, t_c is evaluated for 100 nonadhesive touches and averaged. The total measured adhesion probability, P_t, is determined

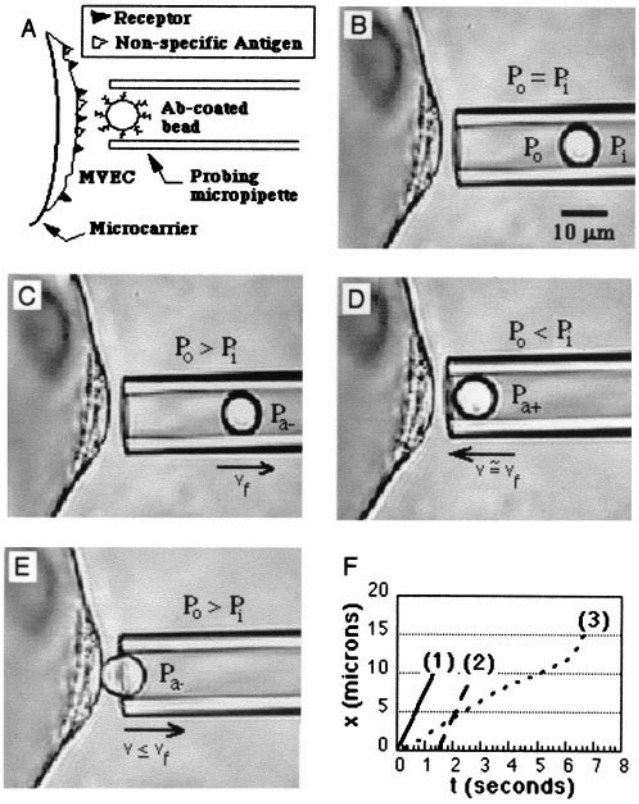

FIGURE 3 Micropipette adhesion assay. (A) The MVEC surface is probed repeatedly with a microsphere coated with mAb to E-selectin. (B-E) Micropipette adhesion assay test cycle, with internal micropipette pressure (P_i) adjusted with respect to media pressure (P_o) to: (B) zero the bead motion, $P_i = P_o$, (C) pull bead into pipette at the free velocity, v_f, with a negative pressure difference, P_{a-}, (D) force the bead to gently contact the cell surface with a positive pressure difference, P_{a+}, and (E) release the bead with P_{a-}. (F) The bead displacement, x, is observed on the video to determine whether the bead: (1) rebounds without adhesion, $dx/dt = v_f$, (2) adheres to the cell, $dx/dt = 0$, followed by detachment, with $dx/dt = v_f$, or (3) adheres and pulls a membrane "tether", with $dx/dt < v_f$.

using linear regressions of cumulative adhesion events, n, against the total number of touches, N, to calculate the slope, P_t, and deviation of the slope (SD) for each cell–bead pair tested. Total adhesion is the sum of specific, Ab–antigen binding, and nonspecific binding to the bead surface. Therefore, data are compensated for nonspecific adhesion as follows:

$$P_a = \frac{(P_t - P_n)}{(1 - P_n)}, \tag{1}$$

where P_n is mean nonspecific adhesion, measured using a nonspecific Ab, P_t is the total measured adhesion, and P_a is the receptor-specific adhesion probability.

Kinetic models

Although receptor expression is measured at discrete time points for thousands of cells, adhesion probability, P_t, is analyzed continuously over small time periods for each cell–bead pair, with tens of cells measured per hour. To correlate these two parameters, adhesion data are grouped in bins according to IL-1α stimulation times at which receptor densities, N_R (μm^{-2}), are assayed by flow cytometry. First, both P_t and N_R are trans-

formed from raw values, which include contributions from nonspecific mAb binding, to specific values. Nonspecific components of binding (P_n) and receptor site measurements are determined using uncoated bead probes in adhesion assays and isotypic Ab in flow cytometry measurements, respectively. Only receptor-positive populations are included in this analysis, defined using the 95th percentile of the nonspecific goat anti-mouse experiment for the adhesion assays and the 95th percentile of the isotype control for flow cytometry, respectively. An exception is made for the unstimulated E-selectin negative control experiments. The unstimulated data mostly falls below the 95th percentile of the nonspecific control, representing a uniform population of cells not separable according to the same criteria. For all data, P_t is compensated for P_n using Eq. 1 to find P_a, and the flow cytometry data are reduced by the mean number of nonspecific receptor sites.

Kinetic models are used to find linear and nonlinear fit parameters for the relationship between P_a and N_R. For $P_a < 30\%$, the probability of forming multiple bonds is insignificant, as demonstrated by Shao and Hochmuth (1999) using Monte Carlo simulations and by Chesla et al. (1998) using analytical solutions to probabilistic models of receptor-mediated cell adhesion (Cozens-Roberts et al., 1990). For single bonds and a negligible bond dissociation rate constant, $k_r \rightarrow 0$, a linear model (Shao and Hochmuth, 1999) is used to find the relationship between P_a and N_R as follows:

$$P_a = KN_R, \tag{2}$$

where

$$K = A_c N_{Ab} t_c k_f. \tag{3}$$

Because bivalent mAb are used to coat the microsphere probes, N_{Ab} (μm^{-2}), the Ab binding site density is twice the number of Ab sites detected using flow cytometry. However, once $P_a > 30\%$, the probability of forming multiple bonds is significant, and Eqs. 2 and 3 do not adequately describe mechanisms involving multiple bonds. Assuming multiple bonds have a Poisson distribution, a nonlinear model,

$$P_a = 1 - \exp(-KN_R), \tag{4}$$

is derived from Chesla et al. (1998). The nonlinear solution, Eq. 4, approaches the linear solution in the limit as $N_R \rightarrow 0$, and the linear solution is a good approximation for $P_a < 30\%$. In the adhesion measurements described here, the adhesion probability is greater than 30% at longer IL-1α stimulation times, and the nonlinear K is used to find k_f using measured values for A_c, N_{Ab}, and t_c.

Statistical analysis

Trends in the adhesion assay are analyzed with a least-squares nonlinear regression (Glantz, 1987), using Mathematica 3.0 software (Wolfram Research, Champaign, IL). Instat 2.0 software (GraphPad Software, San Diego, CA) is used for statistical analysis. The Student's t-test is applied to normally distributed data to determine the significance of differences between parameters found in control and cytokine-induction experiments. When standard deviations are significantly different between sets, Welch's alternate t-test is used instead. For individual sets of flow cytometry data, the Friedman nonparametric test with Dunn's multiple comparison post-test is used to determine the significance of differences. In these cases, data are summarized with descriptive statistics, using percentiles, and compared columnwise with the null hypothesis that all column medians are equal. This test makes no assumptions about the data distribution. Error bars represent SD when data are not normally distributed or SE when sampled data are normally distributed.

RESULTS

Characterization of receptor expression

Figure 4 shows the characteristic pattern of cytokine-induced E-selectin expression in MVEC-L, measured using flow cytometry. IL-1α-stimulated cells exhibit a bimodal pattern of E-selectin expression. The bimodal response persists in MVEC-d deprived of serum or growth factors before stimulation in the E-selectin-positive subset of cells after fluorescence-activated cell sorting and regrowth, and when activated using an alternate cytokine, TNF-α (data not shown). Although the E-selectin-positive fraction is somewhat higher in TNF-α stimulated cells, the E-selectin bimodal response appears to be an intrinsic response of the MVEC, rather than a characteristic of a subset of cells.

Flow cytometry is also used to measure the dose response of E-selectin expressed in cytokine-stimulated MVEC-L. The level of IL-1α is varied to determine an optimal level of cytokine and to minimize the effects of evaporation while the cells are in the chamber. MVEC-L are stimulated for 6 h with 0–300 U/mL IL-1α (Fig. 5). The dose threshold for the induction of E-selectin is 10 U/mL IL-1α, with 11% of the cells E-selectin-positive, and the first significant change in receptor expression occurs at 100 U/mL IL-1α ($p < 0.001$). E-selectin expression peaks at 300 U/mL IL-1α, with 30% ($n = 2$) of the cells E-selectin-positive.

The kinetics of cytokine-induced E-selectin receptor accumulation on MVEC are also measured using quantitative flow cytometry (Fig. 6). MVEC-L are stimulated continu-

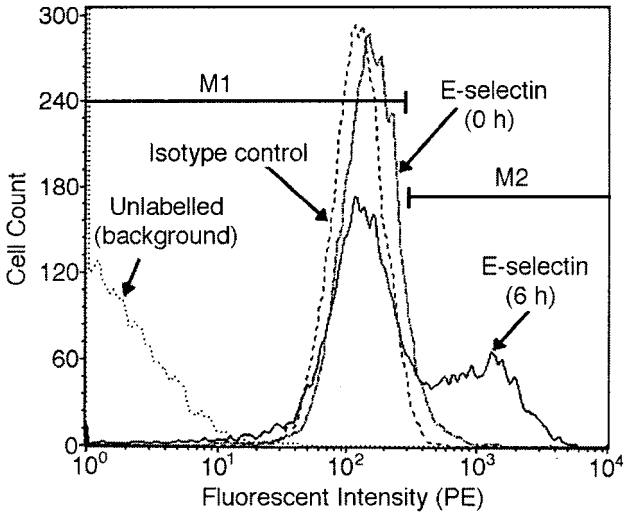

FIGURE 4 Characteristic IL-1α induced E-selectin expression in MVEC-L. Histogram shows the intensity of mAb E-selectin-PE labeled MVEC-L before and after six h of stimulation with 300 U/mL IL-1α, measured using flow cytometry. Gate markers delimit the E-selectin negative (*M1*) and E-selectin positive subsets (*M2*). The isotype control demonstrates that the signal from the unstimulated and E-selectin-negative MVEC-L is produced by nonspecific binding of Ab to the cell surface, and an unlabeled sample of cells demonstrates a low level of autofluorescence.

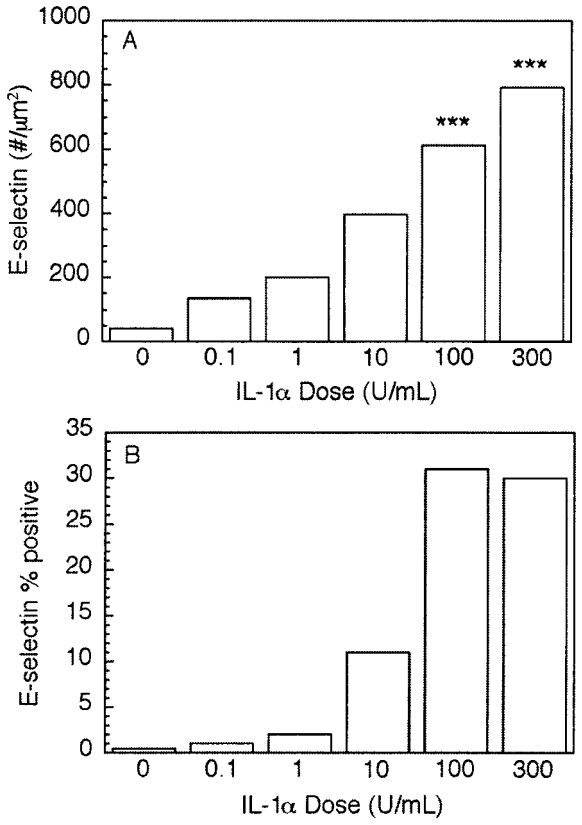

FIGURE 5 Dose response of E-selectin induction by IL-1α in MVEC-L (six h stimulus, n = 10,000). (A) shows E-selectin surface density changes with increasing IL-1α dose for E-selectin positive MVEC-L. Nonspecific binding sites are subtracted from the total. (B) shows the percentage of E-selectin positive MVEC-L detected for each dose tested. P-values (***: $p < 0.001$) are found the Friedman nonparametric test with Dunn's multiple comparison post-test.

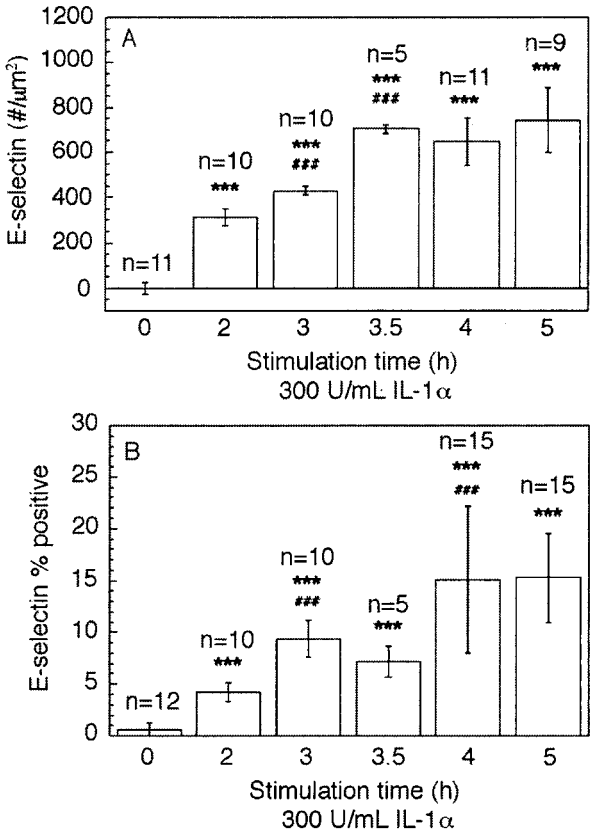

FIGURE 6 Kinetics of IL-1α induced E-selectin expression in MVEC-L, with 0 to five h stimulus. (A) shows E-selectin surface density (μm^{-2}) with nonspecific binding sites subtracted from total number. (B) shows the percentage of receptor-positive cells detected at each interval. Each bar represents mean $\pm$ SD, for flow cytometry tests of separate samples of nominally 10,000 cells each, n = 5–15 as indicated above each bar. P-values are found using t-tests to compare each set of data to the unstimulated, 0 h control (**: $p < 0.01$, ***: $p < 0.001$), and to the preceding time interval, i.e., three h to two h, etc. (###: $p < 0.001$).

ously with 300 U/mL IL-1α for up to 5 h. In IL-1α stimulated data sets, only receptor-positive populations are included in data analysis, and all data sets are compensated for nonspecific Ab binding sites. The density of E-selectin on the cell surface increases with time, peaking to 702 $\pm$ 18 μm^{-2} (mean $\pm$ SD) at 3.5 h, with no statistically significant increase in receptor accumulation up to 742 $\pm$ 143 μm^{-2} at 5 h of IL-1α stimulation (Fig. 6 *A*). The percentage of cells expressing E-selectin peaks after 4 h of IL-1α stimulation at 15 $\pm$ 7% (Fig. 6 *B*).

Characterization of Ab site densities on microspheres

The surface density of Ab (μm^{-2}) on the microsphere probe is measured by saturation binding of two different fluorophore-labeled Abs and quantitative flow cytometry. Aliquots of microspheres are incubated with increasing concentrations of IgG_1-FITC. Binding of the Ab saturates between IgG_1 concentrations 0.625 μg/mL and 2.5 μg/mL, with a density of ~215 μm^{-2}. Similarly, the measurement is made using mAb E-selectin-PE, with saturation of the microspheres at a density of 240 μm^{-2}. In each case, the mean number of actual binding sites per bead is the same. The 10% difference in density estimates is most likely due to inconsistencies between incubation times and temperatures (incubation conditions are one h at 37°C for the anti-E-selectin-PE mAb and overnight at 4°C for the IgG_1-FITC Ab) resulting in changes of nonspecific binding of the Ab to the bead surface. Saturation of sites begins with a loss of linear dependence between Ab concentration and fluorescent intensity and can be determined more conclusively with a plateau in the curve. However, the bead surface provides an infinite number of nonspecific sites, so the curve does not completely plateau, leaving some ambiguity in the measurement. The Ab specificity is unlikely to have any effect on saturation, because the goat anti-mouse sites bind the Fc portion of the mouse Ab. Differences in molec-

ular size are also unlikely to play a role, because the two Ab are both of the IgG_1 subtype.

Characterization of receptor function: E-selectin mediated adhesion

The diameter of contact between cell and bead is measured using video calipers to estimate an $A_c = 3.1 \pm 1.2\ \mu m^2$ ($n = 9$ cell–bead pairs). Within a set of measurements, the variation in A_c is much lower, with SD $\pm$ 0.07 μm^2 (mean of $n = 9$ SD). The measurements are complicated by the difficulty of maintaining the edge of the cell and the edge of the bead within the same focal plane. The surface geometry varies between pairs due to cell curvature and bead orientation, and, although the beads are spherical, each bead has a defect that can obscure precise contact-area measurements.

In two sets of control experiments (Fig. 7) adhesion is measured between goat anti-mouse microspheres and MVEC-L before and after the addition of IL-1α (nonspecific adhesion, Fig. 7 *A*) and between anti-E-selectin-coated microspheres and passive MVEC-L (basal adhesion without cytokine, Fig. 7 *B*). The mean P_n for nonspecific adhesion is 6.5 $\pm$ 7% ($n = 26$), and the mean P_t for E-selectin-mediated adhesion without cytokine stimulus is 12.4 $\pm$ 15.2% ($n = 19$), with statistically insignificant differences between means. Although the E-selectin control gives a response that is apparently higher, this is mostly due to the disproportionate effect of a single cell (see Fig. 7 *B*, cell–bead pair probed after 5 h).

E-selectin-mediated adhesion, induced by IL-1α, began to increase within 1–2 h of stimulation and remained elevated for up to 5 h of stimulation. Fig. 8 shows the results of four separate micropipette assays for adhesion between anti-E-selectin-coated microspheres and cytokine-stimulated MVEC-L, with a pipette suction pressure of 2 pN/μm^2. In three of the assays, E-selectin-mediated adhesion is measured continuously for up to 5 h after the addition of IL-1α to the media (Fig. 8, *A–C*). In the last set, the cells are maintained in the incubator after the application of IL-1α and before testing. In this experiment, E-selectin-mediated adhesion is measured in batches of cells for short periods of up to 2 h (Fig. 8 *D*). The total adhesion probability, P_t, for each cell–bead pair is plotted against the interval of time after initial IL-1α stimulation.

Correlation of expression and function

Qualitatively, stimulus-induced changes in functional measurements of E-selectin correlate with changes in E-selectin expression. The histograms of accumulated E-selectin on cell surfaces of MVEC-L before and after IL-1α stimulation show a large distribution of individual cell response (Fig. 4). Corresponding cell-to-cell heterogeneity is observed in the micropipette adhesion assay (Fig. 8).

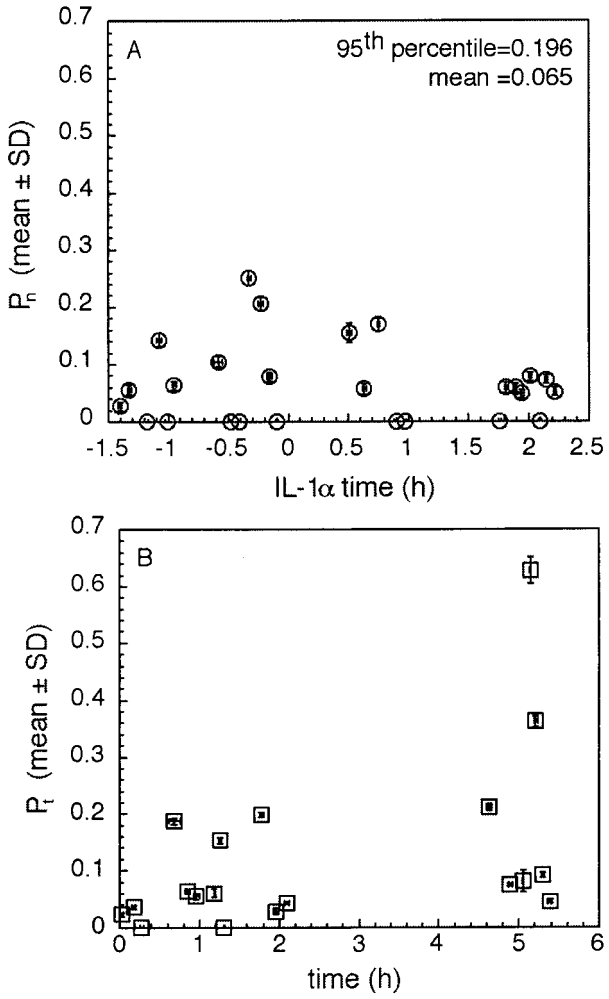

FIGURE 7 Control adhesion assay results: adhesion probability vs. time for each cell-bead pair tested. Error bars represent SD (P_n and P_t) and adhesion test time spans. (A) Nonspecific binding between surfaces is measured using goat anti-mouse beads, before and after the addition of IL-1 α ($n = 26$). The statistics shown, 95th percentile and mean, are used to compensate for nonspecific binding, as described in the text. (B) Adhesion between mAb CD62E-coated beads and passive MVEC-L, measured for up to 5.5 hr in the chamber ($n = 19$).

Parameters P_a and N_R, corrected as described in Materials and Methods, are linked by IL-1α stimulation time. The combined data from Fig. 8 are converted from P_t to P_a (Eq. 1) and grouped in bins of data according to stimulation time (Fig. 9). P_a is plotted against N_R (Fig. 10), and the parameter K is found using a least-square fit to the nonlinear model (Eq. 4) with an R^2 value of 0.949. Eq. 3 is used to calculate the kinetic rate of antibody-E-selectin bond association. This incorporates parameters measured in the adhesion assays (P_a), assayed using flow cytometry (N_{Ab} and N_R) and estimated from video micrographs (A_c and t_c). Because bivalent mAb are used to coat the microsphere probes, N_{Ab} is twice the density of Ab sites detected using flow cytometry. Using flow cytometry measurements, N_{Ab} is found to

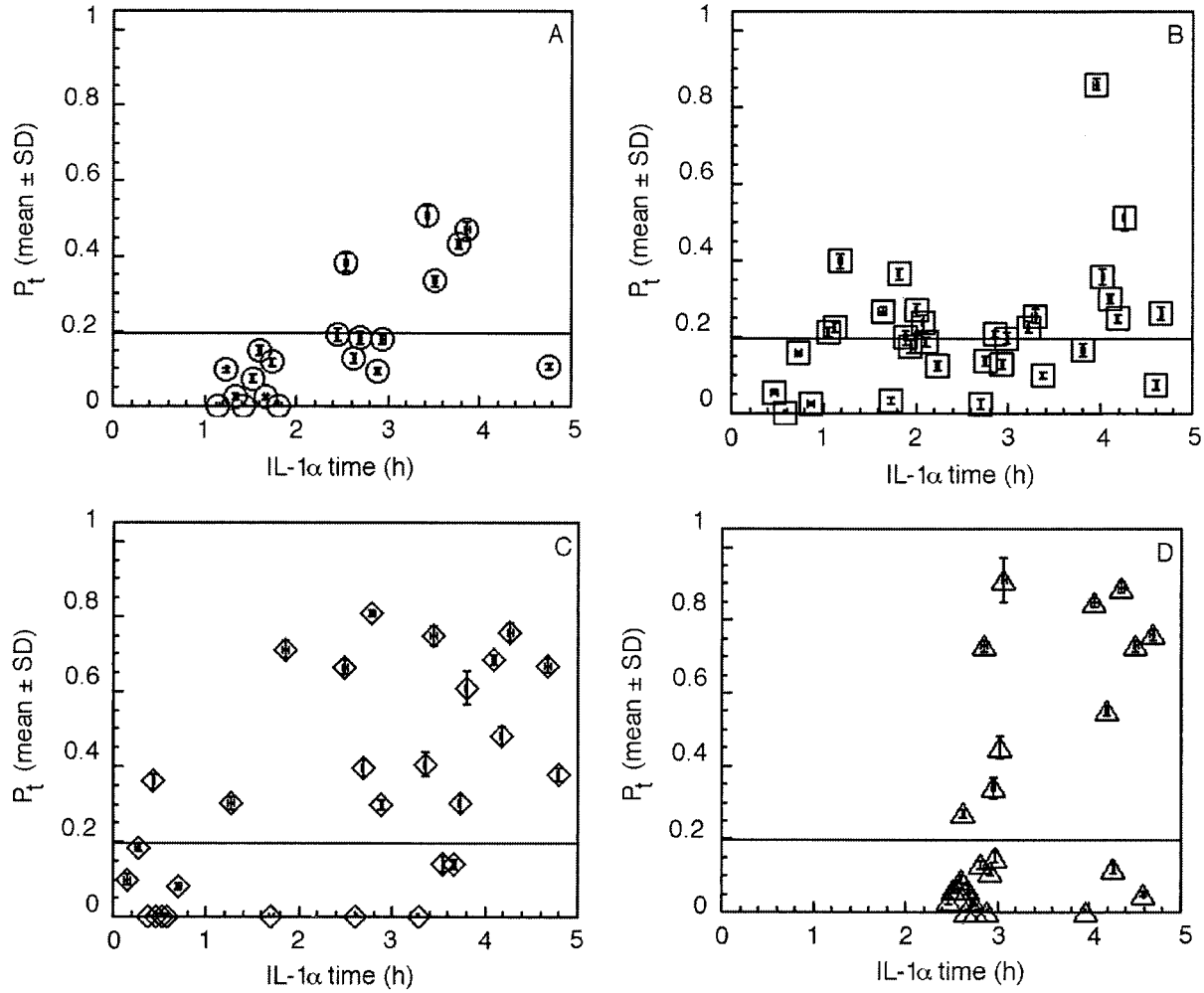

FIGURE 8 Adhesion between mAb CD62E-coated beads and IL-1α-stimulated MVEC-L, shown as P_t for each cell-bead pair tested, $P_t \pm$ SD, against IL-1α exposure time $\pm$ span tested, usually from two - six min. Error bars are in many cases smaller than the symbol. The horizontal line delimits the 95th percentile of the nonspecific control (Fig. 7), above which data are defined as receptor-positive and included in the final analysis of kinetics. (A–C) are separate assays in which batches of cells are tested continuously while MVEC-L are exposed to IL-1α in the micropipette chamber for up to five h. (D) shows the combined results of 4 separate batches of cells probed for shorter periods of time after initial IL-1α exposure.

be 430 μm^{-2}. The estimated contact area, $A_c \cong 3\ \mu m^2$. The contact time, t_c, is 0.25 $\pm$ 0.04 sec (mean $\pm$ SD, $n = 3$). Using Eq. 3 gives $k_f = 3.7 \times 10^{-14}$ cm^2/sec.

DISCUSSION

Temporal patterns of adhesion receptor expression have been studied more extensively in large vessel EC than in microvascular EC, usually using human umbilical EC (HUVEC). Although HUVEC use avoids multiple passaging of cells with tissue available for primary passage, there are significant variations between macro- and microvascular EC in terms of cytokine regulation and receptor expression patterns (Gerritsen et al., 1993; Kansas, 1996). Therefore, we chose MVEC for this study as a good model for the microvascular post-capillary venules, where leukocyte transmigration takes place preferentially in vivo. We observed a bimodal response of E-selectin expression to IL-1α (Fig. 4 and Fig. 6 *B*) with correspondingly nonuniform function (Fig. 8). The bimodal response persisted in MVEC deprived of serum or growth factors, in E-selectin-positive subsets of cells post-FACS, and in TNF-α activated MVEC, with a slightly higher percentage of cells expressing E-selectin with TNF-α induction (data not shown). These findings are consistent with studies of nonuniform E-selectin expression patterns in cytokine-stimulated human brain MVEC (Wong and Dorovini-Zis, 1996). Wong and Dorovini-Zis (1996) showed that the percentage of cells recruited to express E-selectin depends on the cytokine, that TNF-α is more potent than IL-1β, and that between 40–60% of IL-1β induced cells express E-selectin, depending on dosage. Nonuniform expression of adhesion receptors

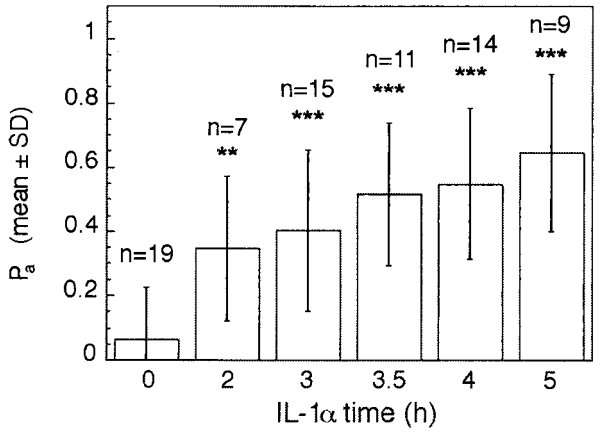

FIGURE 9 Combined E-selectin adhesion data from Fig. 8 with receptor negative subset eliminated, compensated for nonspecific adhesion, and grouped in bins of ± 30 min. Each bar represents mean ± SD for $n = 7$–19 cell-bead pair tests, as indicated above each bar. P-values are found t-tests to compare each set of data to the unstimulated control set (**: $p < 0.01$, ***: $p < 0.001$).

has also been reported for TNF-α stimulated HUVEC monolayers (Munn et al., 1995). Heterogeneity of receptor expression implies that binding of leukocytes is spatially nonuniform, which was in fact observed by Munn et al. (1995), and that the probability of adhesion of beads to cell surfaces deviates acutely about a mean value, as observed here. It is possible that E-selectin induction depends on cell cycle, in addition to cytokine dose and duration, which may be asynchronous within the EC monolayer. This expression pattern may be an artifact of cell culture, but that has no impact on our correlation between expression and function, since we consistently compare MVEC at passage nine. Shen et al. (1995) characterized adhesion receptor expression in MVEC-L grown under similar conditions and found no change in E-selectin expression or induction from passage 3 to passage 12. Since there are significant differences between receptor expression in large vessel and MVEC, further work is necessary to characterize structural and functional determinants of receptor-mediated adhesivity in MVEC.

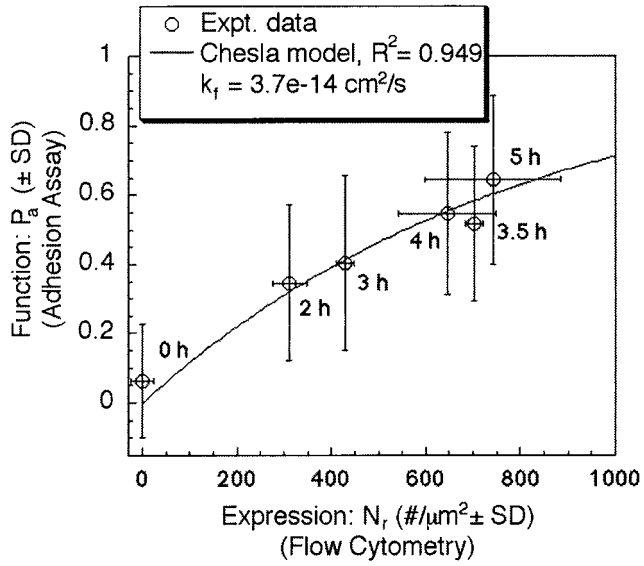

FIGURE 10 Kinetic model fit to experimental data: function vs. expression. Data are compensated for nonspecific Ab binding. Adhesion probabilities, linked by cytokine-stimulation times, are plotted against receptor density data. Data are fit using the nonlinear Chesla model, Eq. 4. Receptor data represent mean ± SD of $n = 5$–11 flow cytometry tests (data shown in Fig. 6), and P_a data represent mean ± SD of $n = 7$–19 cell-bead pairs (data shown in Fig. 9). The forward rate constant is calculated using measured parameters $t_c = 0.25$ sec and $A_c = 3\ \mu m^2$.

In the adhesion assay, a bead is used to repeatedly probe the EC surface. When the Ab-coated bead first contacts the cell surface there are no receptor/ligand bonds. If receptors are available in the contact area, a bond or bonds may form during the contact time t_c. After a bond or bonds form, detachment occurs under the applied force and the bead retracts into the pipette. Whether the mechanism of force-induced detachment between Ab-coated beads and cell surface antigens is receptor extraction, as proposed by Shao and Hochmuth (1999), or Ab-antigen dissociation, the number of receptors and Ab in the contact area remain relatively constant since cell/probe pairs are exchanged within at least 50, but usually within 25 touches. The observed trend of increasing E-selectin mediated adhesion (Fig. 9) corresponds both to published values for rates of E-selectin expression in HUVEC (Kansas, 1996) and to measured rates of E-selectin accumulation on the surface of cytokine-stimulated MVEC (Fig. 6 *A*).

Using simple kinetic models, measured adhesion probabilities are associated with temporally matched receptor densities. The linear model describes first order processes in which only single bonds form, but does not adequately describe mechanisms involving multiple bonds. In the adhesion measurements reported here, P_a exceeds 30% after two h of IL-1α stimulation. Therefore, multiple bonds are given due consideration in the second, probabilistic model for receptor-mediated cell adhesion (Cozens-Roberts et al., 1990). This model is particularly applicable to stochastic systems with small numbers of reacting molecules and deviations about a mean value, as observed in the E-selectin experiments. The probabilistic model was solved analytically by Chesla et al. (1998) for the micropipette adhesion assay. The data fit well to the Chesla model (Eq. 4) with $R^2 = 95\%$, providing a good mechanism for extracting kinetic information. However, the calculated $k_f = 3.7 \times 10^{-14}$ cm^2/sec is several orders of magnitude lower than anticipated.

Several mechanisms besides receptor density contribute to the observed rate of antibody-ligand binding. At 2 pN/μm^2 the detachment force is over 600 pN, 60x the force required to rupture a single bond (Evans et al., 1991). This

suction pressure was chosen to minimize nonspecific binding, but it is entirely possible that the observed P_t excludes undetected bonds that are rapidly extracted. If such a detection error limits the fraction of observed adhesion events, then Eq. 4 is modified as follows:

$$P_a = 1 - \exp[-(1 - \alpha)KN_R], \quad (5)$$

where α is the fraction of false negative adhesions (unobserved events) over a number of touches (Chesla et al., 1998). The most significant consequence of the detection limit is that the forward rate constant is underestimated by a factor of (1 - α). Also as α increases, the probability of having multiple bonds increases at lower apparent adhesion probabilities. In addition to the adhesion detection error, the number of receptors and ligands detected using biochemical measurements is not a completely unambiguous indication of the density of available ligand. It is possible that cytokine-induced changes in microtopology, receptor localization, or clustering play a role in the discrepancies between the predicted and calculated k_f. Immunogold electron microscopy has been used to demonstrate the localization of E-selectin to cytoplasmic projections on TNF-α stimulated brain MVEC (Wong and Dorovini-Zis, 1996). Further studies are necessary to confirm whether this phenomena also occurs with IL-1α stimulation, since there could be significant differences between TNF-α and IL-1α induced receptor localization. Receptor localization to membrane domains such as microvilli on leukocytes or membrane projections on the endothelium tend to amplify adhesion by bringing receptors into closer proximity, but at the same time reduces the effective contact area, and may reduce adhesion if a large percentage of receptors are localized to concave areas.

Because the derived value for k_f is much smaller than what would be expected for intrinsic antibody-antigen binding reactions, $\sim 10^{-9}$–10^{-6} cm^2/sec, the results suggest that the forward rate constant is indeed diffusion-limited. A simple analysis of the contribution of diffusion rates to the overall forward rate constant is instructive. A priori, we assume negligible diffusion of covalently bound Ab on the bead surface. In the diffusion limited case, where $r_+ \gg d_-$, k_f is calculated as follows:

$$k_f = 2\pi D_m(R) \cong 10^{-11}\text{–}10^{-8} \text{ cm}^2/\text{sec}, \quad (6)$$

where r_+ is rate of bond formation, d_- is the rate of diffusion, and $D_m(R)$ is the lateral diffusion constant for the receptor in the membrane (Bell, 1978). In the reaction-limited case, where $r_+ \ll d_-$, the distance between reactants, $R_{R/Ab} \cong 0.75$ nm, and $r_+ \approx 10^6$–10^9 s^{-1} (Bell, 1978), k_f is calculated as follows:

$$k_f = \pi r_+ (R_{R/Ab})^2 \cong 10^{-9}\text{–}10^{-6} \text{ cm}^2/\text{sec}. \quad (7)$$

The value for k_f derived using our data, on the order of 10^{-14} cm^2/sec, is lower than expected for a lateral membrane diffusion-limited process. However, it is an order of magnitude larger than the rates reported by Chesla et al. (1998), $k_f \cong 10^{-15}$ cm^2/sec, with similar effective contact areas. Diffusion of receptors may be limited by steric hindrance or immobilization of the receptors within membrane microdomains. E-selectin may be confined by cytoskeletal linkages or impeded by secondary effects of increased protein concentrations in the cytokine-altered cell membrane: concentrated proteins may increase the membrane viscosity or obstruct lateral diffusion (Jacobson et al., 1987). Since the forward rate constant is largely determined by membrane diffusion, the simple model and experiments presented here offer a useful tool for detecting changes in cytoskeletal attachment.

This is the first study in which a micropipette adhesion assay is used to measure the kinetics of EC receptor binding in vitro. We demonstrate a unique method for extracting kinetic information from measurements of receptor expression and function. This work combines quantitative measurements of adhesion receptor expression and adhesion probability to find an effective two-dimensional association rate constant. The results presented here contribute to a better understanding of the cytokine-induced changes in cell properties that determine the kinetics of adhesion receptor binding. Analyses of the results suggested that cytokine-induced changes in functional adhesion may depend on changing avidity or microtopology of the contact surfaces. This method for extracting kinetic information may be particularly well suited to measuring the kinetics of firm adhesion, mediated by β_2 integrin and ICAM receptors. Based on this method, further studies examining both k_f and k_r for receptor ligand binding, i.e., E-selectin/sLe^x or ICAM-1/LFA-1, would be extremely worthwhile. Adhesion receptors are potentially good targets for antiadhesive therapies to treat systemic diseases of inflammation, in which specific tissues are attacked by the mediators of the immune response (Carlos and Harlan, 1994; Henricks and Nijkamp, 1998; Kavanaugh, 1997). However, further work is necessary to reveal the fundamental relationships between cytokine stimulation and physical and kinetic parameters that determine binding during inflammation.

We would like to thank Dr. Michael Cook and Ms. Lynn Martiniek at the Duke University Comprehensive Cancer Center shared flow cytometry facility. Our thanks also extend to Dr. George Truskey and Dr. Kristina Rinker for their helpful comments and discussions.

This work was supported by grant RO1-HL23728 from the National Institutes of Health.

REFERENCES

Abbassi, O., T. K. Kishimoto, L. V. McIntire, and C. W. Smith. 1993. Neutrophil adhesion to endothelial cells. *Blood Cells.* 19:245–259; discussion 259–260.

Alon, R., S. Chen, K. D. Puri, E. B. Finger, and T. A. Springer. 1997. The kinetics of L-selectin tethers and the mechanics of selectin-mediated rolling. *J. Cell Biol.* 138:1169–1180.

Alon, R., R. C. Fuhlbrigge, E. B. Finger, and T. A. Springer. 1996. Interactions through L-selectin between leukocytes and adherent leukocytes nucleate rolling adhesions on selectins and VCAM-1 in shear flow. *J. Cell Biol.* 135:849–865.

Bell, G. I. 1978. Models for the specific adhesion of cells to cells. *Science.* 200:618–627.

Carlos, T., and J. Harlan. 1994. Leukocyte-endothelial adhesion molecules. *Blood.* 84:2068–2101.

Chen, S., R. Alon, R. C. Fuhlbrigge, and T. A. Springer. 1997. Rolling and transient tethering of leukocytes on antibodies reveal specializations of selectins. *Proc. Natl. Acad. Sci. U.S.A.* 94:3172–3177.

Chesla, S. E., P. Selvaraj, and C. Zhu. 1998. Measuring two-dimensional receptor-ligand binding kinetics by micropipette. *Biophys. J.* 75: 1553–1572.

Cozens-Roberts, C., J. A. Quinn, and D. A. Lauffenburger. 1990. Receptor-mediated cell attachment and detachment kinetics: I. Probabilistic model and analysis. *Biophys. J.* 58:841–856.

Davies, P. F. 1981. Microcarrier culture of vascular endothelial cells on solid plastic beads. *Exp. Cell Res.* 134:367–376.

Davies, P. F., and C. Kerr. 1982. Co-cultivation of vascular endothelial and smooth muscle cells using microcarrier techniques. *Exp. Cell Res.* 141: 455–459.

Erlandsen, S. L., S. R. Hasslen, and R. D. Nelson. 1993. Detection and spatial distribution of the beta 2 integrin (Mac-1) and L-selectin (LECAM-1) adherence receptors on human neutrophils by high-resolution field emission SEM. *J. Histochem. Cytochem.* 41:327–333.

Evans, E., D. Berk, and A. Yeung. 1991. Detachment of agglutinin-bonded red blood cells: I. Forces to rupture molecular-point attachments. *Biophys. J.* 59:838–848.

Evans, E., K. Ritchie, and R. Merkel. 1995. Sensitive force technique to probe molecular adhesion and structural linkages at biological interfaces. *Biophys. J.* 68:2580–2587.

Fritz, J., A. G. Katopodis, F. Kolbinger, and D. Anselmetti. 1998. Force-mediated kinetics of single P-selectin/ligand complexes observed by atomic force microscopy. *Proc. Natl. Acad. Sci.* USA 95:12283–12288.

Gerritsen, M. E., M. J. Niedbala, A. Szczepanski, and W. W. Carley. 1993. Cytokine activation of human macro- and microvessel-derived endothelial cells. *Blood Cells.* 19:325–342.

Glantz, S. A. 1987. Primer of biostatistics. McGraw-Hill Information Services Co., Health Professions Division, New York.

Henricks, P. A. J., and F. P. Nijkamp. 1998. Pharmacological modulation of cell adhesion molecules. *Eur. J. Pharmacol.* 344:1–13.

Huber, A. R., S. L. Kunkel, R. F. d. Todd, and S. J. Weiss. 1991. Regulation of transendothelial neutrophil migration by endogenous interleukin-8. *Science.* 254:99–102.

Jacobson, K., A. Ishihara, and R. Inman. 1987. Lateral Diffusion of Proteins in Membranes. *Ann. Rev. Physiol.* 49:163–175.

Kansas, G. S. 1996. Selectins and their ligands: current concepts and controversies. *Blood.* 88:3259–3287

Kaplanski, G., C. Farnarier, O. Tissot, A. Pierres, A.-M. Benoliel, M.-C. Alessi, S. Kaplanski, and P. Bongrand. 1993. Granulocyte-endothelium initial adhesion: Analysis of transient binding events mediated by E-selectin in a laminar shear flow. *Biophys. J.* 64:1922–1933.

Kavanaugh, A. 1997. Antiadhesion therapy in rheumatoid arthritis - a review of recent progress. *Biodrugs.* 7:119–133.

Kuijpers, T., B. Hakkert, M. Hoogerwerf, J. Leeuwenberg, and D. Roos. 1991. Role of endothelial leukocyte adhesion molecule-1 and platelet-activating factor in neutrophil adherence to IL-1-prestimulated endothelial cells. Endothelial leukocyte adhesion molecule-1-mediated CD18 activation. *J. Immunol.* 147:1369–1376.

Lauffenburger, D. A., and J. J. Linderman. 1993. Receptors: Models for Binding, Trafficking, and Signaling. Oxford University Press, New York.

Levinovitz, A., J. Mühlhoff, S. Isenmann, and D. Vestweber. 1993. Identification of a glycoprotein ligand for E-selectin on mouse myeloid cells. *J. Cell Biol.* 121:449–459.

Lu, H., C. W. Smith, J. Perrard, D. Bullard, L. Tang, S. B. Shappell, M. L. Entman, A. L. Beaudet, and C. M. Ballantyne. 1997. LFA-1 is sufficient in mediating neutrophil emigration in Mac-1-deficient mice. *J. Clin. Invest.* 99:1340–1350.

Lynam, E., L. A. Sklar, A. D. Taylor, S. Neelamegham, B. S. Edwards, C. W. Smith, and S. I. Simon. 1998. Beta2-integrins mediate stable adhesion in collisional interactions between neutrophils and ICAM-1-expressing cells. *J. Leukoc. Biol.* 64:622–630.

Macconi, D., M. Foppolo, S. Paris, M. Noris, S. Aiello, G. Remuzzi, and A. Remuzzi. 1995. PAF mediates neutrophil adhesion to thrombin or TNF-stimulated endothelial cells under shear stress. *Am. J. Physiol.* 269:C42–47.

Marlin, S. D., and T. A. Springer. 1987. Purified intercellular adhesion molecule-1 (ICAM-1) is a ligand for lymphocyte function-associated antigen 1 (LFA-1). *Cell.* 51:813–819.

Merkel, R., P. Nassoy, A. Leung, K. Ritchie, and E. Evans. 1999. Energy landscapes of receptor-ligand bonds explored with dynamic force spectroscopy. *Nature.* 397:50–53.

Munn, L. L., G. C. Koenig, R. K. Jain, and R. J. Melder. 1995. Kinetics of adhesion molecule expression and spatial organization using targeted sampling fluorometry. *Biotechniques.* 19:622–626, 628–631.

Neelamegham, S., A. D. Taylor, A. R. Burns, C. W. Smith, and S. I. Simon. 1998. Hydrodynamic shear shows distinct roles for LFA-1 and Mac-1 in neutrophil adhesion to intracellular adhesion molecule-1. *Blood.* 92: 1626–1638.

Patel K. D. and R. P. McEver. 1997. Comparison of tethering and rolling of eosinophils and neutrophils through selectins and P-selectin glycoprotein ligand-1. *J. Immunol.* 159:4555–4565.

Patel, K. D., K. L. Moore, M. U. Nollert, and R. P. McEver. 1995. Neutrophils use both shared and distinct mechanisms to adhere to selectins under static and flow conditions. *J. Clin. Invest.* 96: 1887–1896.

Piper, J. W., R. A. Swerlick, and C. Zhu. 1998. Determining force dependence of two-dimensional receptor-ligand binding affinity by centrifugation. *Biophys. J.* 74:492–513.

Puri, K. D., E. B. Finger, and T. A. Springer. 1997. The faster kinetics of L-selectin than of E-selectin and P-selectin rolling at comparable binding strength. *J. Immunol.* 158:405–413.

Sako, D., X. J. Chang, K. M. Barone, G. Vachino, H. M. White, G. Shaw, G. M. Veldman, K. M. Bean, T. J. Ahern, and B. Furie et al. 1993. Expression cloning of a functional glycoprotein ligand for P-selectin. *Cell.* 75:1179–1186.

Shao, J.-Y., and R. M. Hochmuth. 1996. Micropipette suction for measuring piconewton forces of adhesion and tether formation from neutrophil membranes. *Biophys. J.* 71:2892–2901.

Shao, J.-Y., and R. M. Hochmuth. 1999. Mechanical anchoring strength of L-selectin, β2 integrins and CD45 to neutrophil cytoskeleton and membrane. *Biophys. J.* 77:587–596.

Shao, J.-Y., H. P. Ting-Beall, and R. M. Hochmuth. 1998. Static and dynamic lengths of neutrophil microvilli. *Proc. Natl. Acad. Sci. U.S.A.* 95:6797–6802.

Shen, J., R. G. Ham, and S. Karmiol. 1995. Expression of adhesion molecules in cultured pulmonary microvascular endothelial cells. *Microvasc. Res.* 50:360–372.

Smith, M. J., E. L. Berg, and M. B. Lawrence. 1999. A direct comparison of selectin-mediated transient, adhesive events using high temporal resolution. *Biophys. J.* 77:3371–3383.

Smith, W. B., J. R. Gamble, I. Clark-Lewis, and M. A. Vadas. 1991. Interleukin-8 induces neutrophil transendothelial migration. *Immunol.* 72:65–72.

Steegmaier, M., A. Levinovitz, S. Isenmann, E. Borges, M. Lenter, H. P. Kocher, B. Kleuser, and D. Vestweber. 1995. The E-selectin-ligand ESL-1 is a variant of a receptor for fibroblast growth factor. *Nature.* 373:615–620.

Tedder, T. F., D. A. Steeber, A. Chen, and P. Engel. 1995. The selectins: Vascular adhesion molecules. *FASEB J.* 9:866–873.

Tonnesen, M. G., D. C. Anderson, T. A. Springer, A. Knedler, N. Avdi, and P. M. Henson. 1989. Adherence of neutrophils to cultured human microvascular endothelial cells. Stimulation by chemotactic peptides and lipid mediators and dependence upon the Mac-1, LFA-1, p150,95 glycoprotein family. *J. Clin. Invest.* 83:637–646.

Webb, W. W., L. S. Barak, D. W. Tank, and E. S. Wu. 1981. Molecular mobility on the cell surface. *Biochem. Soc. Symp.* 46:191–205.

Wong, D., and K. Dorovini-Zis. 1996. Regulation by cytokines and lipopolysaccharide of E-selectin expression by human brain microvessel endothelial cells in primary culture. *J. Neuropathol. Exp. Neurol.* 55: 225–235.

Yang, J., T. Hirata, K. Croce, G. Merrill-Skoloff, B. Tchernychev, E. Williams, R. Flaumenhaft, B. C. Furie, and B. Furie. 1999. Targeted gene disruption demonstrates that P-selectin glycoprotein ligand 1 (PSGL-1) is required for P-selectin-mediated but not E-selectin-mediated neutrophil rolling and migration. *J. Exp. Med.* 190:1769–1782.